Loss of Sigma Factor RpoN Increases Intestinal Colonization of *Vibrio parahaemolyticus* in an Adult Mouse Model

W. Brian Whitaker,[a] Gary P. Richards,[b] E. Fidelma Boyd[a]

Department of Biological Sciences, University of Delaware, Newark, Delaware, USA[a]; United States Department of Agriculture, Agricultural Research Service, Delaware State University, Dover, Delaware, USA[b]

Vibrio parahaemolyticus is the leading cause of bacterial seafood-borne gastroenteritis worldwide, yet little is known about how this pathogen colonizes the human intestine. The alternative sigma factor RpoN/sigma-54 is a global regulator that controls flagellar synthesis, as well as a wide range of nonflagellar genes. We constructed an in-frame deletion mutation in *rpoN* (VP2670) in *V. parahaemolyticus* RIMD2210633, a clinical serogroup O3:K6 isolate, and examined the effects *in vivo* using a streptomycin-treated mouse model of colonization. We confirmed that deletion of *rpoN* rendered *V. parahaemolyticus* nonmotile, and it caused reduced biofilm formation and an apparent defect in glutamine synthetase production. In *in vivo* competition assays between the *rpoN* mutant and a wild-type RIMD2210633 strain marked with the β-galactosidase gene *lacZ* (WBWlacZ), the mutant colonized significantly more proficiently. Intestinal persistence competition assays also demonstrated that the *rpoN* mutant had enhanced fitness and outcompeted WBWlacZ. Mutants defective in the polar flagellum biosynthesis FliAP sigma factor also outcompeted WBWlacZ but not to the same level as the *rpoN* mutant, which suggested that lack of motility is not the sole cause of the fitness effect. In an *in vitro* growth competition assay in mouse intestinal mucus, the *rpoN* mutant also outcompeted the wild type and exhibited faster doubling times when grown in mucus and on individual components of mucus. Genes in the pathways for the catabolism of mucus sugars also had significantly higher expression levels in a Δ*rpoN* mutant than in the wild type. These data suggest that in *V. parahaemolyticus*, RpoN plays an important role in carbon utilization regulation, which may significantly affect host colonization.

Vibrio parahaemolyticus is a Gram-negative bacterium ubiquitous in the marine and estuarine environments worldwide (1–4). *Vibrio parahaemolyticus* is also the leading cause of seafood-associated bacterial gastroenteritis in the United States and Asia (5, 6), which usually stems from the consumption of raw or undercooked shellfish (7, 8). Typically, infection by this organism leads to nausea, vomiting, fever, and a diarrhea distinct from that of the related *Vibrio cholerae*. Less commonly, infection by *V. parahaemolyticus* can cause wound infection and septicemia, leading to mortality in immunocompromised individuals (9–12).

Much effort has gone into understanding the mechanisms that contribute to *V. parahaemolyticus* pathogenesis, with a particular focus on virulence factors produced by this bacterium. Strains that caused disease often possessed either the thermostable direct hemolysin (TDH) or the TDH-related hemolysin (TRH), while nonpathogenic strains typically lacked these two markers (13–15). Additionally, sequence analysis of RIMD2210633, an O3:K6 isolate (TDH$^+$ TRH$^-$), revealed the presence of two type 3 secretion systems (T3SS), one on each chromosome (T3SS-1 and T3SS-2) (16, 17). T3SS-1 is common to both clinical and nonclinical strains of *V. parahaemolyticus* and is a major contributor to cytotoxicity in *in vitro* models (18–22). T3SS-1 is the major contributor to lethality in the intraperitoneal mouse model, and it also plays a minor role in virulence in the infant rabbit model (23). The T3SS-2 gene cluster is flanked by a copy of the *tdh* gene (*tdhA* and *tdhS*) within an 80-kb pathogenicity island named VPaI-7, a region found only in clinical isolates (16, 24–26). T3SS-2 plays only a minor role in cytotoxicity but is the major contributing factor toward enterotoxicity (17, 22, 23, 27). Studies have demonstrated that fluid accumulation in the rabbit ileal loop model as well as virulence in the infant rabbit and infant pig models are dependent upon a functional T3SS-2 (17, 22, 23, 27).

Little is known about how *V. parahaemolyticus* survives within the host gastrointestinal (GI) tract. We recently developed an orogastric adult mouse model that allows for the oral infection and persistent colonization of mice with *V. parahaemolyticus* (28). In conjunction with this model, we also demonstrated that the *Vibrio*-specific two-component regulator ToxRS is an important colonization factor and is required for resistance to acid and bile salt stresses (28). We determined that ToxRS contributes to *in vivo* survival via its regulation of the outer membrane protein OmpU, which is essential for acid and bile salt tolerance (28). It stands to reason that there are a great many other factors that contribute to *V. parahaemolyticus* colonization and survival within the host that have not yet been identified.

Bacteria employ a housekeeping sigma factor, σ^{70} (RpoD), that controls most of the cell's gene expression and a number of alternative sigma factors that typically control a smaller subset of genes with different promoter specificities (29). RpoN (σ^{54}) is one such alternative sigma factor, which in *Escherichia coli* was shown to regulate approximately 30 operons, half of which were involved in nitrogen metabolism (30). The function of RpoN has also been studied in *V. cholerae*, where it was shown to play a role in the regulation of flagellum synthesis, ammonium assimilation, viru-

lence, dicarboxylic acid transport, type VI secretion systems, and quorum sensing (26, 31–36). Studies demonstrated that deletion of *rpoN* in *V. cholerae* leads to aflagellate cells that are nonmotile and are defective for growth on minimal medium where ammonium is the only nitrogen source because of the mutant's inability to express glutamine synthetase (32, 37). Importantly, the *rpoN* mutant exhibited a defect in colonization in the infant mouse model of cholera, and this defect was glutamine synthetase independent and not entirely due to loss of motility (32). Loss of RpoN in other *Vibrio* spp. has also been attributed to loss of motility, reduced biofilm production, and, in the case of *V. fischeri* and *V. anguillarum*, decreased host colonization (38–40).

To the best of our knowledge, this is the first paper to evaluate the role of RpoN in *V. parahaemolyticus* host colonization and survival. Here, we demonstrate that an *rpoN* deletion mutant in *V. parahaemolyticus* colonizes the streptomycin-treated adult mouse model significantly better than the wild-type strain. To determine whether this enhanced fitness effect is due to a lack of motility alone, we constructed in-frame deletions in the sigma factor-encoding genes *fliAP* and *fliAL* and a double deletion in these genes, which produced strains that lacked polar, lateral, or both flagellar systems, respectively. In *in vivo* long-term persistence competition assays, we found that although the *fliAP* mutants but not the *fliAL* mutant outcompeted the wild type, they did not do so to the same level as the *rpoN* mutant. These data indicate that the *rpoN* mutant's enhanced fitness was not due to its role in motility alone. *In vitro* competition assays were performed between wild-type and mutant strains grown on mouse intestinal mucus. In these assays, Δ*rpoN* and Δ*fliAP* outcompeted the wild type and these isolates had a faster doubling time on mucus and its components, suggesting that carbon utilization plays a key role in enhanced fitness *in vivo*.

MATERIALS AND METHODS

Bacterial strains, media, and culture conditions. All strains and plasmids used in this study are listed in Table 1. A previously described streptomycin-resistant *V. parahaemolyticus* RIMD2210633 O3:K6 clinical isolate and a streptomycin-resistant β-galactosidase-positive RIMD2210633 isolate named WBWlacZ were used in this study (28, 41). Unless stated otherwise, all *V. parahaemolyticus* strains were grown aerobically in LB broth (Fisher Scientific, Pittsburgh, PA) containing 3% NaCl at 37°C. For growth studies of all mutants, LB was used as a nutritionally complex medium, while M9 minimal medium (Sigma-Aldrich, St. Louis, MO) was used as a simple medium consisting of salts to which amino acids and carbon sources can be added. M9 medium contains no carbon source but does contain ammonium as the sole nitrogen source that can be converted to glutamine by glutamine synthetase. For experiments analyzing growth characteristics of the Δ*rpoN* strain in M9 medium, the medium was supplemented with 2 mM glutamine unless otherwise stated. Genetic manipulations utilized the *E. coli* diaminopimelic acid (DAP) auxotroph β2155λ pir. The *E. coli* β2155 λpir strain was cultured on medium supplemented with 0.3 mM DAP (Sigma). When required, antibiotics were added to LB broth at the following concentrations: streptomycin, 200 μg/ml; chloramphenicol, 25 μg/ml.

Construction of *V. parahaemolyticus* RIMD2210633 *rpoN*, *fliAP*, *fliAL*, and *fliAP fliAL* deletion mutants. In-frame nonpolar deletions were constructed in the sigma factors encoded by VP2670 (*rpoN*), VP2232 (*fliAP*), and VPA1555 (*fliAL*), and double deletion mutations in *fliAP* and *fliAL* were constructed using splice overlapping extension (SOE) PCR and an allelic exchange method as previously described (28, 41). Briefly, primers were designed to open reading frame (ORF) VP2670, which encodes the alternate sigma factor RpoN, using the *V. parahaemolyticus*

TABLE 1 Bacterial strains and plasmids used in this study

Strain	Genotype or description	Reference or source
Vibrio parahaemolyticus		
RIMD2210633	O3:K6 clinical isolate, Str^r	16, 41
WBWlacZ	RIMD2210633, Str^r, *lacZ*	28
Δ*rpoN*	RIMD2210633 Δ*rpoN* (VP2670), Str^r	This study
Δ*fliAP*	RIMD2210633 Δ*fliAP* (VP2232), Str^r	This study
Δ*fliAL*	RIMD2210633 Δ*fliAL* (VPA1555), Str^r	This study
Δ*fliAP* Δ*fliAL*	RIMD2210633 Δ*fliAP* Δ*fliAL* (VP2232 and VPA1555), Str^r	This study
Δ*rpoN*prpoN	Δ*rpoN* harboring pBBRrpoN	This study
Δ*fliAP*pfliAP	Δ*fliAP* harboring pBBRfliAP	This study
Δ*fliAP* Δ*fliAL*pfliAP	Δ*fliAP* Δ*fliAL* harboring pBBRfliAP	This study
Escherichia coli		
β2155 λpir	Δ*dapA::erm pir*, for bacterial conjugation	
Plasmids		
pDS132	Suicide plasmid, Cm^r, SacB	69
pDSΔrpoN	pDS132 harboring truncated *rpoN* (VP2670) gene	This study
pDSΔfliAP	pDS132 harboring truncated *fliAP* (VP2232) gene	This study
pDSΔfliAL	pDS132 harboring truncated *fliAL* (VPA1555) gene	This study
pBBR1MCS	Expression vector, *lacZ* promoter, Cm^r	
pBBRrpoN	pBBR1MCS harboring full-length *rpoN*	This study
pBBRfliAP	pBBR1MCS harboring full-length *fliAP*	This study

RIMD2210633 genome sequence as the template, and primers were purchased from Integrated DNA Technologies (Coralville, IA) (Table 2). These primers were used to perform SOE PCR and to obtain a 465-bp truncated version of the 1,467-bp *rpoN* gene. The Δ*rpoN* mutant PCR fragment was cloned into the suicide vector pDS132, which was designated pDSΔrpoN. pDSΔrpoN was subsequently transformed into the *E. coli* strain β2155 λpir. pDSΔrpoN was conjugated into *V. parahaemolyticus* RIMD2210633 via cross-streaking on LB plates containing 0.3 mM DAP. Growth from these plates was transferred to LB plates containing 3% NaCl, streptomycin (200 μg/ml), and chloramphenicol (25 μg/ml). The 3% NaCl allowed for optimal *V. parahaemolyticus* growth. The absence of DAP from these plates, plus the addition of chloramphenicol and streptomycin, only selected for *V. parahaemolyticus* cells that harbored pDSΔrpoN. Exconjugate colonies were cultured overnight in LB-3% NaCl without chloramphenicol and were subsequently serially diluted and plated on LB-3% NaCl with 10% sucrose to select for cells which had lost pDSΔrpoN. Double-crossover deletion mutants were screened by PCR using SOEFLrpoNF and SOEFLrpoNR primers and sequenced for verification. The same protocol was used to create in-frame deletion mutations in the alternative sigma factor genes *fliAP* and *fliAL*, as well as *fliAP fliAL*, a double mutation of these genes. We constructed 84-bp and 294-bp truncated versions of the *fliAP* and *fliAL* genes, respectively. All deletions were confirmed to be in-frame via gene sequencing. To ensure the phenotypes observed in this study were not due to disruption of downstream genes, the Δ*rpoN*, Δ*fliAP*, and Δ*fliAP* Δ*fliAL* strains were complemented as described previously (28). Briefly, a full-length copy of the *rpoN* gene was PCR amplified and cloned into the expression vector pBBR1MCS and transferred into the Δ*rpoN* strain, designated Δ*rpoN*prpoN. Assays utilizing the Δ*rpoN*prpoN strain were routinely supplemented with 100 mM isopropyl-β-D-thiogalactopyranoside (IPTG). This process was repeated for the Δ*fliAP* and Δ*fliAP* Δ*fliAL* strains. Complementation primers can be found in Table 2.

Motility assay. Motility assays were conducted on either LB containing 2% NaCl and 0.3% agar for swimming motility assays or heart infusion (HI) (Remel, Lenexa, KS) plates containing 2% NaCl and 1.5% agar for swarming motility assays. For swim assays, a single colony was picked from a fresh plate using a sterile pipette tip and stabbed into LB containing 0.3% agar. Plates were incubated overnight at 37°C, and images of each

TABLE 2 Primers used in this study

Primer name and use	Sequence (5′–3′)[a]	Melting temp (°C)	Product (bp)
Splice overlap extension PCR			
SOEvp2670A	<u>TCT AGA</u> TTA TCT CGG CGA ACA ATT CC	56	315
SOEvp2670B	GAT TTC TGT TGG CTC GTT GG	43	
SOEvp2670C	CCA ACG AGC CAA CAG AAA TCT TCT CCA GCC ACG TCA GTA C	67	302
SOEvp2670D	<u>GAT ATC</u> TGC ATT GAA TCG GTA AGA TCA	55	
SOEvp2670FlFor	GAC TCA AAC CCG CTA TTG GA	55	1,325
SOEvp2670FlRev	TGA CTT GAA GGG GCA ATA CC	55	
SOEvp2232A	<u>TCT AGA</u> GCG TTG ATC GAG GTT GAA CT	59	756
SOEvp2232B	AAC GTT TAC GCA CCA AGC TC	56	
SOEvp2232C	GAG CTT GGT GCG TAA ACG TTT AAA CTT GCC ATG CTG GTC	66	609
SOEvp2232D	<u>GAG CTC</u> AAC TTC TGG CAC ACA AAG CA	61	
SOEvp2232FlFor	ACG CGA CGA ATA ATT TGA CC	53	2,831
SOEvp2232FlRev	TGC CAG TGG CTT ACA TAG CA	57	
SOEvpa1555A	AAT CTA GAC AGA CGC ACT TTG TCA TGC T	60	411
SOEvpa1555B	ATG AAC GCG AAG TTG GTT AA	53	
SOEvpa1555C	TTA ACC AAC TTC GCG TTC ATC GAC TGT CAA AGC GAG ATC A	66	453
SOEvpa1555D	<u>AAG AGC TCA</u> ACT TGA AAC CAC GGC TAC G	62	
SOEvpa1555FlFor	GGT GAA ACC AGC TCA CTG CT	58	1,450
SOEvpa1555FlRev	TTC TGG TGC TTC GAT GTG AG	55	
Complement primers			
rpoNforward	<u>GGT ACC</u> TGA GCA TTA CAA GGT AAG TAA CAC TG	60	1,500
rpoNreverse	<u>TCT AGA</u> AGT GCC TTA AAG TAG GCG TTT	58	
fliAPforward	<u>CCC GGG</u> TCG CAG AGG ACC CTT TTG	66	753
fliAPreverse	<u>TCT AGA</u> TTA GTC ATT TTG TGT CCA CGC AC	59	
RT-PCR primers			
VP0063For	TCA ACT CCA TAT CGC CAT CA	54	219
VP0063Rev	CAC GAG CGA ACA TTC AGA AA	53	
VPA1674For	ATG CCT GGT TCA AAA ACG T	53	211
VPA1674Rev	CCT TTA GAG CGC TGG TTT GC	55	
VPA1083For	CCT TTT GCA CCG AGA GTG AT	55	222
VPA1083Rev	TGT GGC AAA AGA TGC AAA AA	52	
VPA1425For	TGA GAT CAT GGC GAA CTC AG	55	210
VPA1425Rev	GTT CGT TGG TTG GCT TGT TT	54	

[a] Underlined base pairs indicate restriction sites.

plate were taken the following day. Swarming assays were performed similarly, with the exception that the strains were inoculated only onto the surface of the HI-1.5% agar plates using sterile pipette tips. These plates were incubated at 30°C for 60 h before images were taken.

Electron microscopy. The wild-type and Δ*rpoN* strains were analyzed for their ability to produce flagella using transmission electron microscopy. Strains were grown either in LB-3% NaCl broth or on an HI plate with 2% NaCl. Cells were adhered to a Formvar/carbon grid (Electron Microscopy Sciences, Hatfield, PA) and negatively stained with 1% phosphotungstate. Images were taken using a Zeiss LIBRA transmission electron microscope.

Biofilm assay. *Vibrio parahaemolyticus* wild-type and mutant strains were grown overnight at 37°C aerobically in LB broth with 3% NaCl. Overnight cultures were diluted 1:40 in fresh LB-3% NaCl and allowed to grow statically in a 96-well plate for 24 h. After static incubation, the culture was decanted and each well was washed once with sterile phosphate-buffered saline (PBS) to remove any loosely adherent cells. Crystal violet (Electron Microscopy Sciences) was added to each well at a concentration of 0.1% (wt/vol) and incubated at room temperature for 30 min. The crystal violet was decanted, and each well was washed once with sterile PBS. Crystal violet that stained adhering cells (biofilm) was solubilized with dimethylsulfoxide (DMSO), and the optical density at 595 nm (OD_{595}) of each well was measured using a Tecan Sunrise microplate reader and Magellan plate reader software (Tecan Systems Inc., San Jose, CA).

Mouse streptomycin pretreatment and inoculation preparation. All experiments involving mice were approved by the University of Delaware Institutional Animal Care and Use Committee. Male C57BL/6 mice, aged 6 to 10 weeks, were housed under specific-pathogen-free conditions in standard cages in groups (4 per group) and provided standard mouse feed and water *ad libitum*. Treatment with streptomycin and inoculations were performed as previously described (28). In essence, mice were fasted for 4 h and then orogastrically administered 20 mg streptomycin per mouse (100 μl of streptomycin at 200 mg/ml). Food and water were returned upon antibiotic treatment. Twenty hours after antibiotic treatment, the mice were fasted for 4 h and then inoculated with a 100-μl bacterial suspension in PBS by gavage. Water was returned immediately upon infection, and food was returned 2 h postinfection. *Vibrio parahaemolyticus* inocula were prepared from wild-type RIMD2210633 and WBWlacZ, Δ*rpoN*, Δ*fliAP*, Δ*fliAL*, and Δ*fliAP*Δ*fliAL* mutant cultures grown aerobically overnight in LB supplemented with 3% NaCl and streptomycin (200 μg/ml) at 37°C. The WBWlacZ strain used in competition experiments, as described below, is RIMD2210633 with a β-galactosidase gene knock-in, as previously described (28). This strain is designated WBWlacZ and substitutes for the wild-type strain in coinfections, which allows for color selection of the WBWlacZ strain (blue colonies) against a background of mutants (white colonies). These overnight cultures were diluted 1:50 with LB streptomycin and grown aerobically at 37°C for 4 h. An aliquot of the 4-h bacterial culture was pelleted and washed once with sterile PBS before being resuspended in fresh PBS to a final concentration of $\sim 1 \times 10^{10}$

CFU/ml. Each inoculum was serially diluted and the titers determined on LB streptomycin plates to determine the dose administered.

***In vivo* competition assays.** Inocula for competition assays were prepared as described above, with the following modifications. Four-hour cultures of wild-type, WBWlacZ, Δ*rpoN*, Δ*fliAP*, Δ*fliAL*, and Δ*fliAP* Δ*fliAL* strains were pelleted by centrifugation at 4,000 × *g*, washed with PBS, and centrifuged again. The resulting bacterial pellet was resuspended in PBS to a concentration of approximately 1 × 10^{10} CFU/ml based on the culture OD$_{600}$. A 1-ml aliquot of each deletion mutant strain was combined with 1 ml of the WBWlacZ strain, yielding a bacterial suspension of 1 × 10^{10} CFU/ml with a ratio of 1:1 CFU of mutant to WBWlacZ strain. A bacterial suspension of 1 × 10^{10} CFU/ml with a ratio of 1:1 CFU of wild-type to WBWlacZ strain was also examined in all experiments. The inoculum was serially diluted and plated on plates of LB agar containing 3% NaCl plus streptomycin and 120 μg/ml 5-bromo-4-chloro-3-indolyl-β-D-galactopyranoside (X-Gal) to determine the exact ratio in the inocula. Mice were prepared by following the streptomycin treatment protocol outlined above. Mice were inoculated with 100 μl of the appropriate bacterial suspension as previously described. In order to evaluate strain persistence within the mouse intestine, fresh fecal pellets (2 to 4 per animal) were collected at daily intervals. The pellets were weighed and then placed in 2 ml of sterile PBS for mechanical homogenization. Diluted samples were plated for CFU on LB agar containing 3% NaCl plus streptomycin and X-Gal for a blue (WBWlacZ) versus white (wild-type or deletion mutant strain) screen of colonies after incubation at 37°C overnight. In a separate experiment, mice were treated and infected as described above and then sacrificed 24 h postinfection, and the entire gastrointestinal tract was harvested from each mouse. Samples were placed in 8 ml of sterile PBS, mechanically homogenized, serially diluted in PBS, and plated on LB-3% NaCl plus streptomycin and X-Gal for CFU determination. *In vitro* competition assays were performed in tandem with the *in vivo* assays by diluting the inoculum 1:50 into fresh LB-3% NaCl broth. This culture was incubated at 37°C for 24 h and then serially diluted and plated on LB agar with 3% NaCl and X-Gal. The competitive index (CI) was determined with the following equation: CI = ratio out$_{(mutant/wild-type)}$/ratio in$_{(mutant/wild-type)}$. A CI of >1 indicates that the test strain has the ability to outcompete the wild-type strain, while a CI of <1 indicates that the test strain is less fit than the wild-type strain. "Ratio out" refers to the ratio of deletion mutant to WBWlacZ colonies recovered from the mouse intestine, while "ratio in" refers to the ratio of the deletion mutant to WBWlacZ colonies enumerated from the inoculum.

Bacterial localization. To elucidate where in the gastrointestinal tract *V. parahaemolyticus* was colonizing, the small intestine, cecum, and large intestine were analyzed separately for colonizing bacteria. Mice and inocula were prepared as outlined above. Streptomycin-treated mice were infected with either the wild-type strain or the Δ*rpoN* strain. Twenty-four hours postinfection, mice were sacrificed by CO$_2$ asphyxiation, and the entire gastrointestinal tract was removed and separated into the small intestine, cecum, and large intestine. Individual organs were placed into 4 ml of sterile PBS, mechanically homogenized, and serially diluted in PBS. Serially diluted samples were plated for CFU on LB-streptomycin selection plates and incubated at 37°C overnight.

Mucus extraction. Intestinal mucus was extracted from the gastrointestinal tract of mice as follows. Mice were orally treated with streptomycin as outlined above to mimic the *in vivo* mouse experiments. Twenty-four hours after antibiotic treatment, mice were sacrificed by CO$_2$ asphyxiation and their GI tracts were dissected. Mucus was collected by flushing the cecum with PBS to remove its contents and then by gently scraping the walls of the intestine to remove the mucus. Extracts from small intestine, cecum, or large intestine were also collected. Extracted mucus was stored at −80°C until further use. For growth assays, 200 mg of mucus was diluted in 5 ml of PBS, homogenized, and centrifuged for 10 min at 500 × *g* to pellet out tissue and fecal materials. To determine the ability of strains to utilize mucus as a sole carbon source, the small intes-

tine, cecum, or large intestine mucus was added to M9 medium at a final concentration of 30 μg of protein/ml (42, 43).

Mucus and carbon utilization. *Vibrio parahaemolyticus* strains (wild type and WBWlacZ, Δ*fliAP*, Δ*fliAL*, and Δ*fliAP*Δ*fliAL* mutants) were grown overnight in M9 medium supplemented with 3% NaCl and 0.4% glucose (M9G medium), and the Δ*rpoN* strain was grown in M9G supplemented with 2 mM glutamine to compensate for the defect in the mutant's ability to utilize ammonium present in M9 as a sole nitrogen source (32). Overnight cultures were pelleted by centrifugation for 10 min at 4,000 × *g*. Bacterial pellets were washed once with M9 and then resuspended in M9 with no carbon source. Cultures were diluted 1:40 into fresh M9 supplemented with 3% NaCl and either gluconate (0.4%), ribose (0.4%), arabinose (0.4%), mannose (0.4%), glucose (0.4%), or mouse intestinal mucus (30 μg/ml). The *rpoN* mutant in these experiments was also supplemented with 2 mM glutamine. Diluted cultures were transferred to a 96-well microtiter plate and incubated at 37°C with shaking. Optical densities at 595 nm were taken hourly for a total of 24 h using a Tecan Sunrise microplate reader and Magellan plate reader software. Doubling times for each strain and carbon source were calculated by dividing the time interval used (min) by the number of generations (*n*): *n* = ln(OD2/OD1)/ln2, where OD1 is the optical density of the culture at the start of the log phase and OD2 is the optical density of the culture at the end of the log phase. Each experiment was performed in triplicate with at least two biological replicates.

RNA extraction and qPCR. *Vibrio parahaemolyticus* strains were grown for 4 h in LB-3% NaCl and then diluted 1:50 into M9 medium containing no ammonium and supplemented with cecal mucus as a sole carbon and nitrogen source. For these experiments, in order to best mimic *in vivo* conditions, M9 was made without the addition of ammonium. Therefore, in these experiments all bacterial strains tested were forced to utilize the supplemented mucus as the sole carbon and nitrogen source. To determine expression patterns of carbon metabolism genes in mucus, we examined early-exponential-phase cultures; therefore, all cultures were grown to an OD$_{595}$ of 0.15. Total RNA was extracted using TRIzol (Invitrogen, Carlsbad, CA) according to the manufacturer's protocols. The RNA samples were quantified using a Nanodrop spectrophotometer (Thermo Scientific, Waltham, MA) and subsequently treated with Turbo DNase (Invitrogen) per the manufacturer's instructions. cDNA was synthesized using Superscript II reverse transcriptase (RT) (Invitrogen) according to the manufacturer's protocol, using 500 ng of RNA as a template and priming with 200 ng of random hexamers. cDNA samples were then diluted 1:25 and used for quantitative real-time PCR (qPCR). Real-time PCRs used the HotStart-IT SYBR green qPCR master mix (USB, Santa Clara, CA) and were run on an Applied Biosystems 7500 fast real-time PCR system (Foster City, CA). Gene-specific primers were designed using Primer 3 software according to the real-time PCR guidelines and are listed in Table 2. Data were analyzed using Applied Biosystems 7500 software. Expression levels of each gene, as determined by their cycle threshold (C_T) values, were normalized using the 16S rRNA gene to correct for sampling errors. Differences in the ratios of gene expression were determined using the ΔΔC_T method (44).

Mucus competition assays. *In vitro* competition assays were performed in mouse intestinal cecal mucus. Mixed cultures containing the WBWlacZ strain and test strains were prepared by following the mouse inoculum protocol outlined above. Intestinal mucus was diluted to a final concentration of 30 μg/ml of protein in M9 medium containing no ammonium. Again, for these experiments, the ammonium was removed from the M9 medium so that neither the wild type nor the deletion mutants had an advantage over the *rpoN* mutant, which is defective in utilizing ammonium as a nitrogen source. Forcing the bacteria to rely solely on the supplied mucus for carbon and nitrogen also closely mimics the conditions experienced by the strain in the mouse intestine. Mixed cultures of wild-type and deletion mutant strains were then diluted 1:50 into the M9 (no ammonium) medium supplemented with mucus and incubated aerobically overnight at 37°C. After 24 h, cultures were serially diluted and
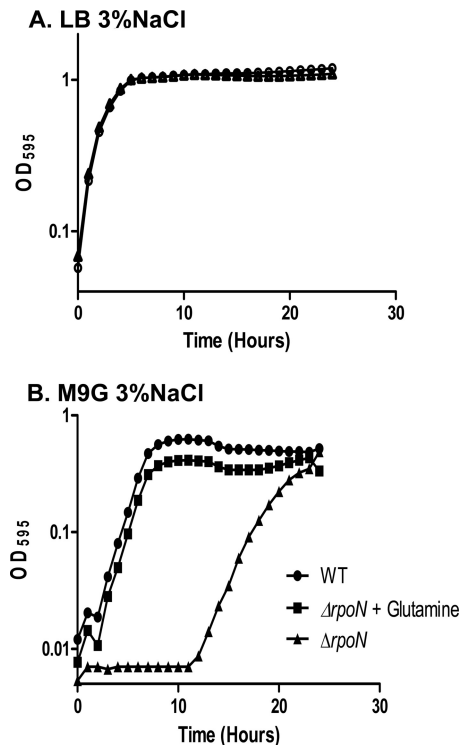
A. LB 3%NaCl

B. M9G 3%NaCl

FIG 1 Growth characteristics of wild-type and Δ*rpoN* strains. (A) Both the wild-type (circle) and Δ*rpoN* (triangle) strains were grown aerobically at 37°C in LB medium with 3% NaCl. (B) Both the wild-type (circle) and Δ*rpoN* (triangle) strains were grown aerobically at 37°C in M9 minimal medium with 3% NaCl and 0.4% glucose (M9G). Additionally, the Δ*rpoN* strain was also grown in M9G plus 2 mM glutamine (square). All cultures were grown in triplicate, and each experiment was performed at least twice. Error bars, indicating standard deviations, are too small to be observed.

plated on LB-3% NaCl plus X-Gal, and the CI values were calculated as outlined above. For these experiments the *rpoN* mutant cultures were not supplemented with glutamine; thus, they were grown similarly to the other deletion mutant strains where the supplied mucus served as the sole carbon and nitrogen sources.

RESULTS

Growth analysis of Δ*rpoN* strain. RpoN has been shown to be a global regulator in a number of Gram-negative bacteria, where it is known to regulate motility, nitrogen assimilation, quorum sensing, and virulence (30–33, 37–40, 45, 46). VP2670 encodes the RpoN homologue in *V. parahaemolyticus* RIMD2210633 and shared 81% identity with RpoN (VC2529) from *V. cholerae* N16961. To determine the role of this regulator in *V. parahaemolyticus* pathogenesis, we constructed an in-frame deletion in VP2670. We created an unmarked 465-bp truncated version of the *rpoN* gene in *V. parahaemolyticus* RIMD2210633 using SOE PCR and homologous recombination.

To ensure that the *rpoN* mutant had no general growth defects, we compared growth of the mutant to that of the wild-type strain grown under standard laboratory conditions (LB-3% NaCl) and found that the Δ*rpoN* strain exhibited no defects in growth relative to the wild-type parent strain (Fig. 1A). We also compared the growth of the Δ*rpoN* strain to that of the wild-type strain in an M9G medium and found that the Δ*rpoN* strain exhibited a substantial lag phase of approximately 11 h compared to the wild-type

strain before reaching the same biomass as the parent strain (Fig. 1B). To demonstrate that the growth of the mutant in M9G was not the result of a suppressor mutation, we took cells of the *rpoN* mutant grown overnight in M9G and inoculated them into new media and found a similar lag time with these cultures. The 11-h lag phase could be reduced to the wild-type level by the addition of 2 mM glutamine to the medium (Fig. 1B). This suggests that the *V. parahaemolyticus rpoN* mutant has a defect in the synthesis of glutamine synthetase (encoded by VP0121), an enzyme that synthesizes glutamine from the ligation of glutamate and ammonia. While RpoN deletions in some Gram-negative bacteria result in glutamine auxotrophy (46–48), our data suggest that RpoN is important but not absolutely necessary, since delayed growth of the *rpoN* mutant was observed in minimal medium with ammonium as the sole nitrogen source. This phenotype is also observed in other *Vibrio* species, such as *V. cholerae*, *V. fischeri*, and *V. alginolyticus* (32, 38, 40), which implies that in *Vibrio* spp., glutamine synthetase is basally transcribed independent of RpoN. However, under certain conditions, such as growth in M9G medium containing ammonium as a sole nitrogen source, RpoN is required for maximal expression of glutamine synthetase.

RpoN controls swimming and swarming motility in *V. parahaemolyticus* RIMD2210633. The role of RpoN in the regulation of flagellar synthesis has been studied in a number of *Vibrio* species (32, 38–40, 49, 50). *Vibrio parahaemolyticus* produces both a polar flagellum for movement through liquid medium (swimming) and a lateral flagellar system for movement over solid surfaces (swarming) (49, 50). We compared the ability of the wild-type and the *rpoN* mutant strains to swim and swarm. A colony of the wild-type strain stabbed onto LB plates containing 0.3% agar and incubated overnight showed the initial inoculum spreading throughout the plate, which is indicative of swimming (Fig. 2A). However, when a colony of the Δ*rpoN* strain was examined under the same conditions, there was no movement beyond the initial inoculum site (Fig. 2A). These data confirm that the *rpoN* mutant does not have the ability to swim in this medium. Similarly, when a colony of the wild-type strain was inoculated onto HI-1.5% agar plates and incubated, the colony growth expanded in an asymmetrical pattern, indicative of swarming behavior. In contrast, when the Δ*rpoN* strain was examined under the same conditions, the Δ*rpoN* colonies that formed were round and symmetrical, which indicates that this strain does not have the ability to swarm (Fig. 2A). Additionally, we compared the ability of the wild-type and Δ*rpoN* strains to produce flagella under both swimming (Fig. 2B) and swarming (Fig. 2C) conditions and confirmed that no flagella were produced in the *rpoN* mutant. The defects in swimming and swarming in the Δ*rpoN* mutant are due to the loss of polar and lateral flagella, respectively, as indicated by transmission electron microscopy (Fig. 2B and C).

We also examined the effects of deletion of the *rpoN* gene on the bacterium's ability to form biofilms. We found that the Δ*rpoN* and Δ*fliAP* Δ*fliAL* strains produced significantly less (*P* < 0.01) biofilm than the wild-type strain after static growth for 24 h in LB-3% NaCl (Fig. 2D).

Loss of RpoN enhances *V. parahaemolyticus* RIMD2210633 colonization. Studies on a number of enteric pathogens have shown that motility is an important phenotype for colonization and infection (32, 33, 39, 40, 51–54). To determine whether RpoN was essential for colonization in *V. parahaemolyticus* pathogenesis, we used the streptomycin-treated mouse model of colonization (28).

A Colony phenotypes
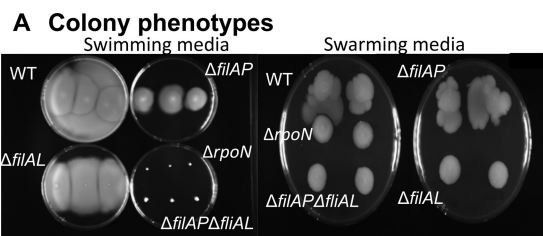
B Swimming (LB 2% NaCl 0.3% agar)
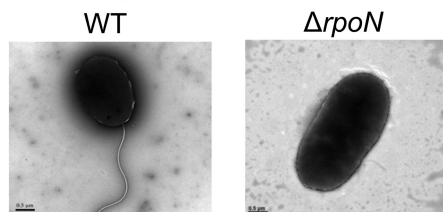
C Swarming (HI 2% NaCl 1.5% agar)
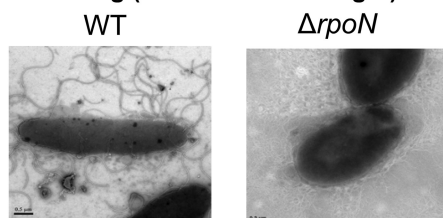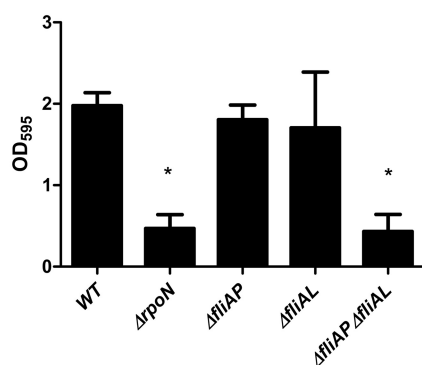

D Biofilm Formation

FIG 2 Examination of motility, flagellar synthesis, and biofilm production of *V. parahaemolyticus* RIMD2210633 and an *rpoN* deletion mutant. (A) To examine the motility phenotypes of the Δ*rpoN*, Δ*fliAP*, Δ*fliAL*, and Δ*fliAP* Δ*fliAL* strains, bacterial colonies were stabbed onto an LB plate containing 2% NaCl and 0.3% agar to assess swimming. Plates were incubated at 37°C, and photographs were taken after 24 h. To examine swarming, strains were grown on the surface of a heart infusion plate containing 2% NaCl and 1.5% agar. The plates were incubated at 30°C, and photographs were taken after 60 h. Electron microscopy was used to examine the production of polar and lateral flagella in wild-type and Δ*rpoN* mutant strains grown in swimming (B) and swarming (C) media. (D) To examine biofilm production, the wild-type strain and sigma factor deletion mutants were grown overnight aerobically in LB supplemented with 3% NaCl at 37°C. Overnight cultures were diluted into fresh LB-3% NaCl and allowed to grow statically for 24 h at 37°C in a 96-well plate. After such time, the culture was removed and adherent cells were stained with crystal violet. The crystal violet was solubilized in DMSO, and the OD_{595} was determined. Bars represent the OD_{595} of each strain. All cultures were grown in triplicate, and each experiment was performed at least twice. Error bars indicate standard errors. *P* values were calculated using an unpaired Student *t* test with a 95% confidence interval. Asterisks denote significant differences between biofilm production of the mutant strains and that of the wild-type strain. *, $P < 0.01$.
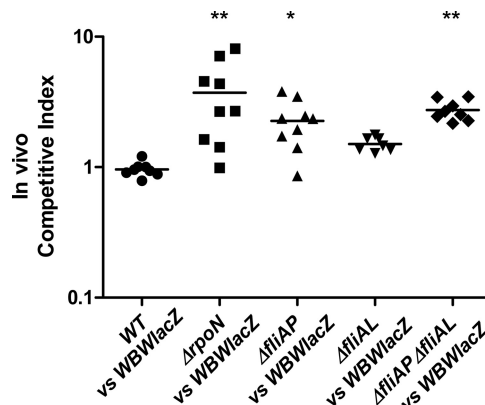

FIG 3 *In vivo* competition assays. A 1:1 mixed culture of WBWlacZ and test strain (wild type or deletion mutants) was used to orogastrically infect streptomycin-treated adult mice. CFU were calculated 24 h postinfection from the entire gastrointestinal tracts using blue/white colony selection. Data are pooled from two separate experiments and reported as competitive index (CI), which is calculated as CI = ratio out$_{(test strain/WBWlacZ)}$/ratio in$_{(test strain/WBWlacZ)}$. The solid lines indicate the means. *P* values were calculated using a Kruskal-Wallis one-way ANOVA followed by a Dunn multiple-comparison posttest. Asterisks denote significant differences between the CI of the mutant strains and that of the wild-type strain. *, $P < 0.05$; **, $P < 0.01$.

For this analysis, a β-galactosidase-positive RIMD2210633 strain named WBWlacZ was used, which was previously demonstrated to behave similarly to the wild type *in vitro* and *in vivo* (28). We examined the ability of WBWlacZ and the *rpoN* mutant to cocolonize the intestinal tract of streptomycin-pretreated adult mice. An *in vivo* competition assay in adult C57BL/6 mice was performed by pretreating mice with an orogastric dose of streptomycin (20 mg/mouse) 24 h prior to orogastric coinoculation with a mixture of 5×10^8 CFU *V. parahaemolyticus* WBWlacZ and 5×10^8 CFU of either the wild-type strain (*n* = 8) or the Δ*rpoN* mutant (*n* = 9). The wild-type and WBWlacZ strains did not outcompete each other *in vivo* (CI = 0.96) (Fig. 3), indicating that insertion of the *lacZ* gene is neither deleterious nor beneficial, confirming previously reported values (28). In *in vitro* assays, the wild-type versus WBWlacZ strain comparison had a CI of 1, as previously shown (28). Conversely, the *rpoN* mutant significantly (*P* < 0.01) outcompeted the WBWlacZ strain by 3.8-fold *in vivo* (Fig. 3). This indicates that the Δ*rpoN* strain has increased fitness *in vivo* compared to the wild-type strain.

In vitro competition assays were performed between these strains in LB broth, and in these assays WBWlacZ outcompeted the *rpoN* mutant with a CI of 0.25 (Fig. 4A). We believe that this defect *in vitro* most likely is a result of the Δ*rpoN* strain's defect in glutamine synthetase and that this defect is exacerbated when it must compete with WBWlacZ under *in vitro* conditions. To examine this further, *in vitro* competition assays were performed in LB supplemented with glutamine. In this assay, the mutant made a recovery but was still outcompeted by the WBWlacZ strain (Fig. 4A). To mimic *in vivo* conditions more closely, *in vitro* competition assays were performed in M9 (with and without ammonium) supplemented with intestinal mucus. For these assays, the ability of *V. parahaemolyticus* to grow on mouse intestinal mucus as a sole nutrient source was first assessed. Mucus is the main component of mucous membranes and is the primary source of nutrients for most intestinal microbiota (55, 56). We collected mucus from
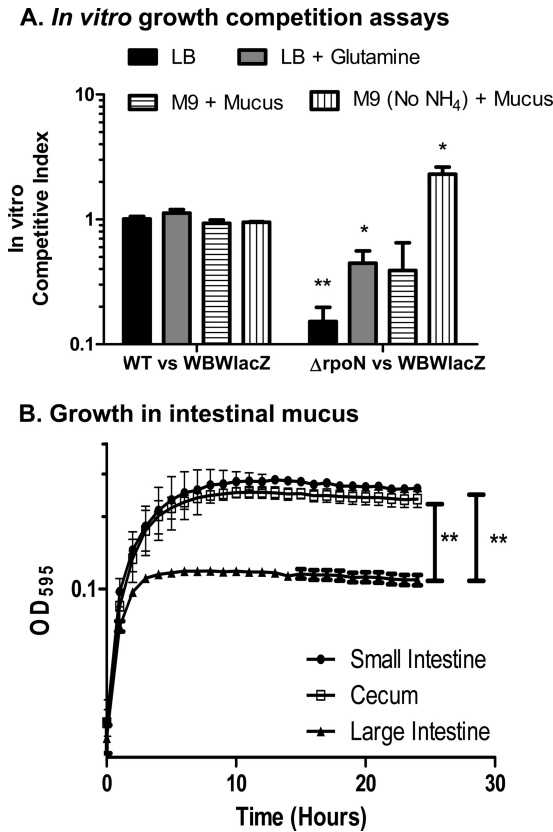
A. *In vitro* growth competition assays

B. Growth in intestinal mucus

FIG 4 *V. parahaemolyticus in vitro* competition assays and growth in mouse intestinal mucus. (A) *In vitro* competition assays showing competitive indices in LB-3% NaCl broth with and without 2 mM added glutamine or in M9 3% NaCl medium supplemented with mucus either with or without ammonium as the nitrogen source. (B) Wild-type *V. parahaemolyticus* was grown overnight at 37°C aerobically in M9 3% NaCl supplemented with either small intestine mucus (circles), cecal mucus (squares), or large intestine mucus (triangle), and growth was determined for 24 h at OD_{595}. All mucus samples were adjusted to contain 30 μg/ml of protein. The final OD_{595} was used to compare the growth potential on each substrate. Error bars indicate standard errors. *P* values were calculated using an unpaired Student *t* test with a 95% confidence interval. Asterisks denote significant differences between the competitive index of the Δ*rpoN* strain and the competitive index of the wild-type strain (A) or the final OD_{595} of the wild-type strain grown utilizing mucus isolated from the small intestine, cecum, or large intestine (B). *, $P < 0.05$; **, $P < 0.001$.

streptomycin-treated mice from the small intestine, cecum, and large intestine to mimic *in vivo* conditions used in this study. In *in vitro* competition assays, *V. parahaemolyticus* was grown overnight in M9 supplemented with small intestine, cecum, or large intestine mucus (30 μg/ml of mucus protein) as a sole carbon source at 37°C. Growth occurred on all three mucus extracts, but the bacterium grew to significantly higher optical densities on M9 supplemented with either small intestine mucus or cecal mucus compared to its growth on large intestine mucus ($P < 0.001$) (Fig. 4B). In M9 supplemented with mucus, the *rpoN* mutant was outcompeted but not to the same extent as in LB (Fig. 4A). In M9 medium (no ammonium) supplemented with mucus, the *rpoN* mutant was able to outcompete the WBWlacZ strain with a CI of 2.3 (Fig. 4A). These results suggest that both strains obtain nitrogen from mucus and that the glutamine synthetase defect in the Δ*rpoN* strain does not play a significant role *in vivo*.

To begin to determine how the *rpoN* mutant outcompeted the

wild-type strain *in vivo*, we performed single-infection *in vivo* mouse colonization experiments to compare the localization of the Δ*rpoN* mutant to that of the wild-type strain. Streptomycin-treated mice were given an oral dose of 1×10^9 CFU of either the wild-type or Δ*rpoN* strain. Twenty-four hours postinfection, the mice were sacrificed and their small intestine, cecum, and large intestine were harvested separately and plated for CFU. We found that the Δ*rpoN* strain colonized the mouse small intestine at an approximately 2.5-fold higher level than the wild type ($P < 0.05$). However, there was no significant difference ($P > 0.05$) between the amount of Δ*rpoN* and WBWlacZ strains recovered from the cecum and large intestine (1.2- and 1.6-fold, respectively) (data not shown).

We next examined whether the superior ability of the Δ*rpoN* strain to colonize the mouse intestine was dependent upon the inability of the Δ*rpoN* strain to synthesize polar, lateral, or both flagellar systems. In *V. parahaemolyticus*, the sigma factor FliAP is required for the synthesis of the single-sheath flagellum and requires sodium motive force to swim in liquid media (49, 57). FliAL, encoded by *lafS*, regulates the synthesis of the lateral flagella, which requires energy from the proton motive force to drive swarming motility on solid media (50, 58, 59). We examined the expression level of *fliAP* in the *rpoN* mutant background and, as expected, we found highly reduced expression (data not shown). In order to test whether a lack of polar or lateral flagella alone played a role in the superior colonization of the *rpoN* mutant, we constructed single deletion mutations in *fliAP* (VP2232) and *fliAL* (VPA1555) sigma factor genes and in a double mutant lacking *fliAP* and *fliAL* genes. As expected, we confirmed that the Δ*fliAP* strain did not produce a polar flagellum and was defective in swimming motility but exhibited the same phenotype as the wild-type strain on swarming plates (Fig. 2A). The Δ*fliAL* strain exhibited wild-type levels of swimming motility but was unable to swarm, whereas the double deletion mutant showed defects in both swim and swarm motility (Fig. 2A). Neither the Δ*fliAP* nor Δ*fliAL* strain exhibited defects in the ability to produce biofilm. However, as previously mentioned, the Δ*rpoN* and Δ*fliAP* Δ*fliAL* strains were defective in biofilm production compared with the wild-type strain ($P < 0.01$) (Fig. 2D), indicating that motility, either by polar or lateral flagella, is important for biofilm production and that a defect exhibited by the Δ*rpoN* mutant in biofilm production may be motility related.

The colonization ability of the Δ*fliAP*, Δ*fliAL*, and Δ*fliAP* Δ*fliAL* strains was determined *in vivo* via competition assay using our streptomycin-treated adult mouse model. Like the Δ*rpoN* strain, the Δ*fliAP* and Δ*fliAP* Δ*fliAL* strains were able to significantly outcompete the WBWlacZ strain, with Δ*fliAP* and Δ*fliAP* Δ*fliAL* strains having competitive indices of 2.3 ($P < 0.05$) and 2.7 ($P < 0.001$), respectively (Fig. 3). The *fliAL* mutant was not significantly different from the WBWlacZ strain. Under *in vitro* conditions, all 3 motility mutant strains were found to have a CI close to 1. Even though the polar mutants outcompeted WBWlacZ *in vivo*, they did not do so to the same level as the *rpoN* mutant, suggesting that other factors are involved in its superior colonization.

The RpoN mutant shows superior colonization in long-term persistence competition assays compared to WBWlacZ. To determine whether the deletion mutants exhibit different phenotypes during the later stages of colonization, *in vivo* long-term persistence assays in the mouse intestine were performed. To ac-
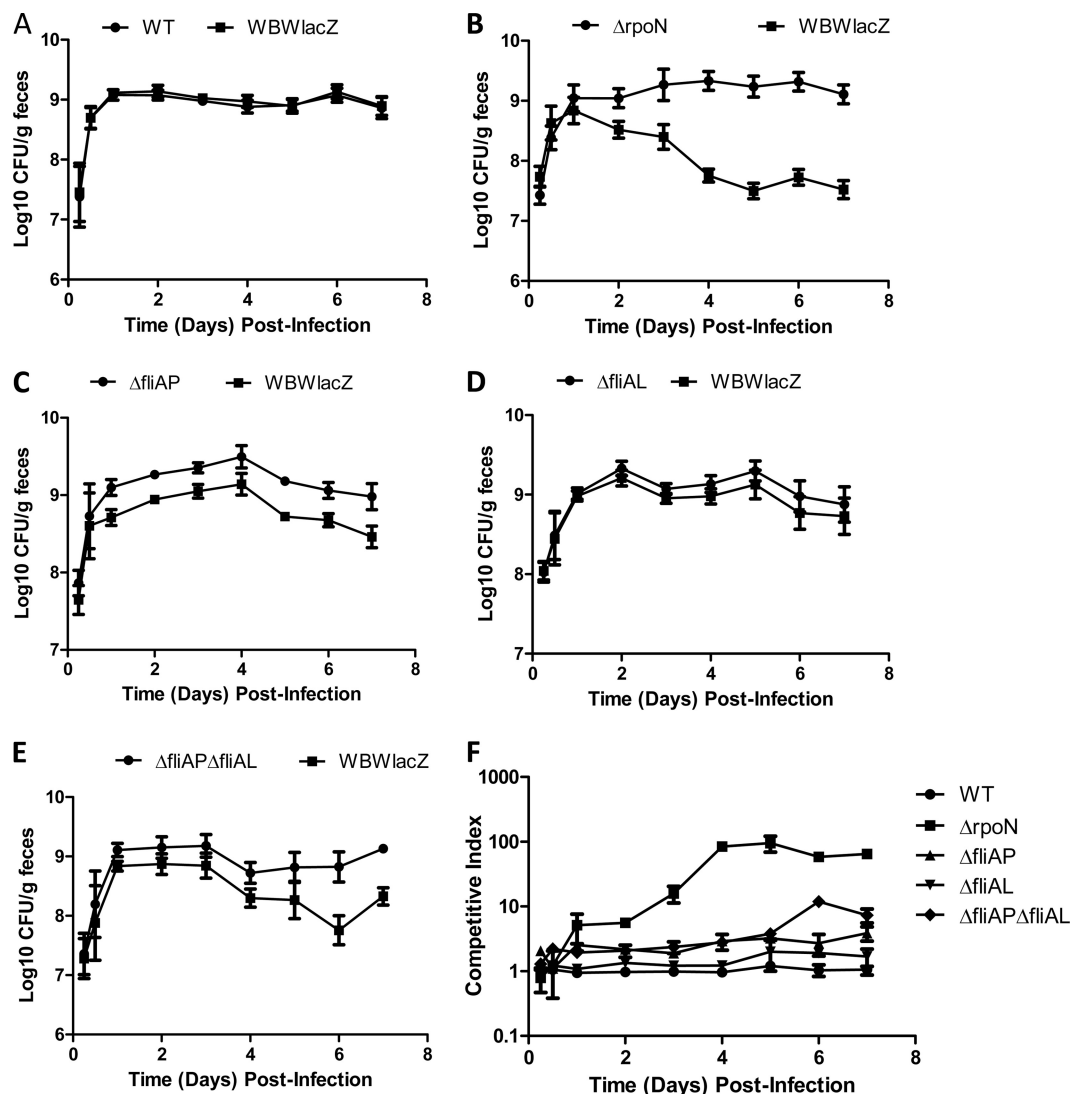
FIG 5 *In vivo* persistence competition assays. Groups of streptomycin-treated mice were orally dosed with a mixed inoculum consisting of the WBWlacZ strain and either the wild-type (A), Δ*rpoN* (B), Δ*fliAP* (C), Δ*fliAL* (D), or Δ*fliAP* Δ*fliAL* (E) strain. At the indicated intervals postinfection, fecal pellets were collected from mice, weighed, and homogenized in PBS. Samples were serially diluted and plated on LB agar containing 3% NaCl and X-Gal to determine the number of *V. parahaemolyticus* organisms per gram of fecal material. Data are pooled from two separate experiments and reported as log-transformed CFU/gram of feces (A to E) or as the competitive index (F), which is calculated as CI = ratio out$_{(test\ strain/WBWlacZ)}$/ratio in$_{(test\ strain/WBWlacZ)}$. Error bars indicate standard errors.

complish this, streptomycin-treated mice were coinfected with WBWlacZ and either the wild-type, Δ*rpoN*, Δ*fliAP*, Δ*fliAL*, or Δ*fliAP* Δ*fliAL* strain. The *Vibrio* levels within the intestine were monitored by collecting and subsequently plating feces from infected mice daily for 7 days. This experiment confirmed that the Δ*rpoN*, Δ*fliAP*, and Δ*fliAP* Δ*fliAL* mutants (Fig. 5B, C, and E) were able to outcompete the WBWlacZ strain starting at 24 h postinfection and continuing through day 7. There was no significant difference between the wild-type and WBWlacZ strain at any point during the 7 days of fecal monitoring (Fig. 5A and F). Similarly, a comparison of WBWlacZ to Δ*fliAL* strains exhibited a CI of approximately 1 at 24 h and throughout the 7 days, indicating that in this model, lateral flagella are not required for colonization (Fig. 5D and F). In the 7-day persistence assays, the Δ*rpoN* strain was significantly more fit in the mouse intestine than any of the other strains tested, exhibiting a CI shift from approximately 2 at

24 h postinfection to approximately 70 at 7 days postinfection (Fig. 5B and F). The Δ*fliAP* strain outcompeted the WBWlacZ strain with a CI of approximately 3 through the 7 days in the mouse intestine (Fig. 5C and F). The Δ*fliAP* Δ*fliAL* strain outcompeted the WBWlacZ strain with a competitive index of approximately 10 by 7 days postinfection (Fig. 5E and F). These results suggest that the lack of FliAP and a polar flagellum gives a competitive advantage *in vivo*. However, in all *in vivo* experiments, the Δ*rpoN* strain outcompeted the WBWlacZ strain at much higher levels than either the Δ*fliAP* or Δ*fliAP* Δ*fliAL* strains, suggesting that while loss of motility likely contributes to the colonization phenotype of all three strains, it is clear that RpoN controls additional factors that are important for host colonization.

Growth in mouse intestinal mucus and mucus components. One of the barriers to pathogen colonization of the gut for many species is competition from the resident microbial populations for
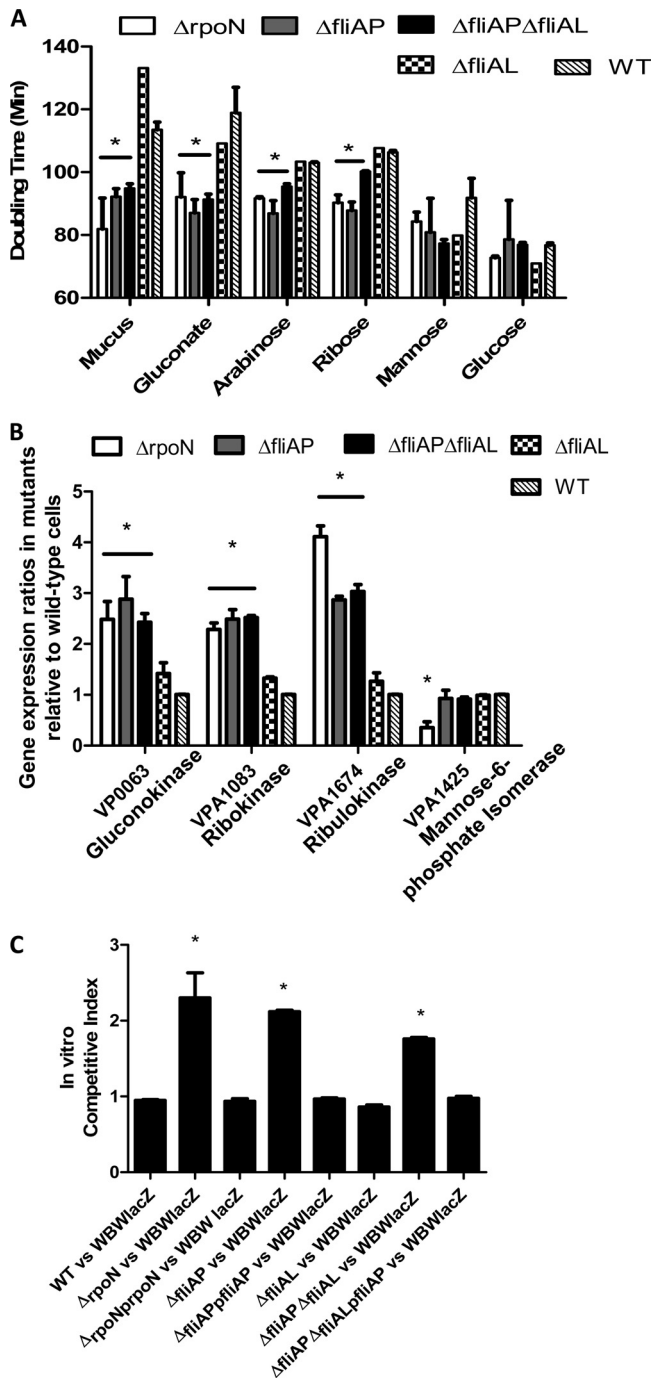
FIG 6 Growth characteristics of *V. parahaemolyticus* on cecal mucus. (A) Doubling times of wild-type and mutant strains. Overnight cultures of the Δ*rpoN*, Δ*fliAP*, Δ*fliAP*Δ*fliAL*, Δ*fliAL*, and wild-type strains were grown aerobically in M9 medium supplemented with either cecal mucus (30 μg/ml of protein), gluconate (0.4%), mannose (0.4%), arabinose (0.4%), ribose (0.4%), or glucose (0.4%) for 24 h, and growth was determined at OD_{595}. Doubling times were calculated as mentioned in Materials and Methods. (B) Expression analysis of wild-type and mutant strains. RNA was extracted on two separate occasions from wild-type and mutant Δ*rpoN*, Δ*fliAP*, Δ*fliAL*, and Δ*fliAP* Δ*fliAL* cells grown in cecal mucus and analyzed by qPCR in duplicate for each biological replicate. Bars represent the expression of the gluconokinase (VP0063), ribokinase (VPA1083), ribulokinase (VP1674), and mannose-6-phosphate isomerase (VPA1425) normalized to 16S rRNA and are relative to levels in the wild-type cells. (C) *In vitro* competitive indices of strains grown on mucus. Mixed cultures of WBWlacZ and Δ*rpoN*, Δ*fliAP*, Δ*fliAL*, Δ*fliAP*

nutrients (60, 61). We hypothesized that one of the ways our *rpoN* mutant is outcompeting WBWlacZ is by the more efficient *in vivo* utilization of carbon sources. To explore this, the doubling time of each of the mutants was examined in M9 supplemented with mucus where, for the *rpoN* mutant assays, glutamine was also added to M9. The Δ*rpoN*, Δ*fliAP*, Δ*fliAP*Δ*fliAL*, Δ*fliAL*, and wild-type strains exhibited average doubling times of 81.9 min, 92.2 min, 94.3 min, 130.0 min, and 113.5 min, respectively (Fig. 6A). The doubling times for the Δ*rpoN*, Δ*fliAP*, and Δ*fliAP*Δ*fliAL* strains were significantly faster ($P < 0.05$) than those for the wild-type strain (Fig. 6A).

To ascertain if any of the individual major carbon components in mucus were contributing more than others to the mutants' superior growth, we compared the growth of all strains in M9 medium supplemented with gluconate, arabinose, ribose, mannose, or glucose as the sole carbon source, and for the *rpoN* mutant assays, glutamine was also added to M9 (Fig. 6A). When cells were grown in M9 medium with gluconate as the sole carbon source, the Δ*rpoN*, Δ*fliAP*, and Δ*fliAP*Δ*fliAL* strains had average doubling times of 92.1 min, 87.0 min, and 91.3 min, respectively, which were significantly faster ($P < 0.05$) than the 118.9-min doubling time of the wild-type strain (Fig. 6A). More similar to the wild-type strain, the Δ*fliAL* strain had a doubling time of 107.9 min ($P > 0.05$). When cells were grown using arabinose as the sole carbon source, the Δ*rpoN*, Δ*fliAP*, and Δ*fliAP*Δ*fliAL* strains had average doubling times of 91.2 min, 86.8 min, and 95.4 min, respectively, which were significantly faster ($P < 0.05$) than the 104.8-min and 103.2-min doubling times of the Δ*fliAL* and wild-type strains, respectively (Fig. 6A). With ribose as the sole carbon source, the Δ*rpoN*, Δ*fliAP*, and Δ*fliAP* Δ*fliAL* strains had average doubling times of 90.5, 87.8, and 100.0 min, respectively, which were again significantly shorter ($P < 0.05$) than those of the Δ*fliAL* and wild-type strains, with average doubling times of 110.9 and 106.3 min, respectively (Fig. 6A). We found no significant difference between the generation times of the wild-type strain and the mutant strains when grown in minimal medium containing glucose or mannose as sole carbon sources (Fig. 6A). Taken together, these data demonstrate that the Δ*rpoN*, Δ*fliAP*, and Δ*fliAP* Δ*fliAL* strains have higher growth rates than the wild-type strain when grown on mucus, and these strains also exhibit higher growth rates on gluconate, arabinose, and ribose as sole carbon sources, which are the major carbon sources present in mucus.

Loss of RpoN and FliAP derepresses key metabolic genes. Given that the Δ*rpoN*, Δ*fliAP*, and Δ*fliAP* Δ*fliAL* strains had higher growth rates in mouse intestinal mucus as well as in a number of carbon sources commonly present in mucus, we hypothesized that these sigma factors act as repressors of certain metabolic pathways. Therefore, the expression patterns of genes encoding gluconokinase (VP0063), ribokinase (VPA1083),

---

Δ*fliAL*, or complemented strains were grown for 24 h in M9 medium supplemented with cecal mucus. The competitive index for each strain relative to the WBWlacZ strain was calculated. Each experiment was performed in triplicate with at least two replicates. Errors bars indicate standard errors. *P* values were calculated using an unpaired Student *t* test with a 95% confidence interval. Asterisks denote significant differences between the doubling times of the mutant strains and the doubling times of the wild-type strain (A), gene expression in the mutant strains relative to the wild-type strain (B), or competitive index of mutant strains compared to the competitive index of the wild-type strain (C). *, $P < 0.05$.

ribulokinase (VPA1674), and mannose-6-phosphate isomerase (VPA1475), required for gluconate, ribose, arabinose, and mannose catabolism, respectively, were examined during growth in mucus. For these expression experiments, M9 lacking both ammonium and glutamine was used for all strains examined, ensuring the only source of nitrogen for all strains was mucus. Higher expression was found for the genes encoding the metabolic enzymes gluconokinase, ribokinase, and ribulokinase for the hypercolonizing mutants than for the wild type (Fig. 6B). Gluconokinase (encoded by VP0063) catalyzes the conversion of D-gluconate to 6-phospho-D-gluconate, which can then be shuttled to the pentose phosphate pathway or the Entner-Doudoroff pathway. We analyzed expression levels of this gene in both the wild-type strain and the mutant strains grown to an OD of 0.15 in M9 supplemented with mucus. The expression levels were approximately 2.5-, 2.9-, and 2.8-fold higher in the $\Delta rpoN$, $\Delta fliAP$, and $\Delta fliAP$ $\Delta fliAL$ strains, respectively, than in the wild-type strain ($P < 0.05$) (Fig. 6B). Ribokinase (encoded by VPA1083) is the enzyme responsible for converting D-ribose to D-ribose-5-phosphate, which can be utilized by the cell via the pentose phosphate pathway. The expression levels of this gene were approximately 2.3-, 2.5-, and 2.5-fold higher in the $\Delta rpoN$, $\Delta fliAP$, and $\Delta fliAP$ $\Delta fliAL$ strains, respectively ($P < 0.05$), compared to the wild-type strain (Fig. 6B). Ribulokinase (encoded by VPA1674) catalyzes the conversion of L-ribulose (which is generated via the isomerization of L-arabinose) into L-ribulose-5-phosphate, which is then converted into an intermediate of the pentose phosphate pathway. Expression of this gene was approximately 4-, 2.9-, and 3-fold higher in the $\Delta rpoN$, $\Delta fliAP$, and $\Delta fliAP$ $\Delta fliAL$ strains, respectively ($P < 0.05$), than in the wild-type strain (Fig. 6B). These expression data suggest that when grown in intestinal mucus, the $\Delta rpoN$, $\Delta fliAP$, and $\Delta fliAP$ $\Delta fliAL$ strains are exhibiting higher expression of genes in the pathways for the catabolism of gluconate, arabinose, and ribose than the wild-type strain. This could mean that in wild-type cells, either RpoN or FliAP acts, either directly or indirectly, as a repressor for these metabolic pathways. Furthermore, the higher expression patterns seen in these pathways in the $\Delta rpoN$, $\Delta fliAP$, and $\Delta fliAP$ $\Delta fliAL$ strains could explain the higher growth rates (lower doubling times) observed when these strains were grown using mucus, gluconate, arabinose, and ribose as sole carbon sources and why the mutant strains can outcompete the WBWlacZ strain both *in vitro* and *in vivo*. Mannose-6-phosphate isomerase (encoded by VPA1425) catalyzes the isomerization of mannose-6-phosphate to fructose-6-phosphate. This allows cells to utilize mannose as a carbon source via glycolysis. We found no significant alteration in expression of this gene in the $\Delta fliAP$ and $\Delta fliAP$ $\Delta fliAL$ strains compared to wild-type expression levels (Fig. 6B). However, expression of VPA1425 was significantly decreased ($P < 0.05$) in the $\Delta rpoN$ strain, indicating that RpoN acts as a positive regulator of mannose catabolism. The $\Delta fliAL$ strain, which exhibited no difference in growth rates in mucus, did not exhibit significant differences in metabolic gene expression relative to the wild-type strain (Fig. 6B).

To assess whether the faster doubling time and increased expression of catabolic genes in mucus of the hypercolonizers leads to a competitive advantage, we performed *in vitro* competition assays in M9 medium supplemented with intestinal mucus. For these experiments, M9 medium lacked ammonium and glutamine for all assays, so that the bacteria were forced to derive nitrogen solely from the mucus. In these experiments, the $\Delta rpoN$,

$\Delta fliAP$, and $\Delta fliAP$ $\Delta fliAL$ strains were able to outcompete ($P < 0.05$) the WBWlacZ strain approximately 2.3-, 2.1-, and 1.8-fold, respectively (Fig. 6C). Furthermore, when the $\Delta rpoN$, $\Delta fliAP$, and $\Delta fliAP$ $\Delta fliAL$ strains were complemented with functional genes, they lost the ability to outcompete the WBWlacZ strain for growth utilizing mucus as the sole nutritional source (Fig. 6C).

DISCUSSION

In an effort to better understand how *V. parahaemolyticus* colonizes and survives within the host, we examined a strain where the alternative sigma factor RpoN was deleted. We confirmed that loss of RpoN renders *V. parahaemolyticus* aflagellate and nonmotile, causing a defect in biofilm formation and likely a defect in the synthesis of glutamine from glutamate and ammonium. We also demonstrated that the $\Delta rpoN$ strain has the ability to significantly outcompete WBWlacZ *in vivo* in a streptomycin-treated adult mouse model of colonization. Additionally, other mutant strains defective for polar flagellar synthesis, $\Delta fliAP$ and $\Delta fliAP$ $\Delta fliAL$ strains, also demonstrated enhanced fitness *in vivo* but not to the same extent as the *rpoN* mutant. This was also true in persistence colonization assays performed over 7 days, which again showed that the $\Delta rpoN$ strain significantly outcompeted WBWlacZ. These results suggested that the $\Delta rpoN$ *in vivo* phenotype is not due in any large part to a lack of motility. In *in vitro* competition assays in minimal medium using intestinal mucus as the sole nutritional source, the *rpoN*, *fliAP*, and *fliAP* *fliAL* mutants outcompeted WBWlacZ but not to the same extent as in the *in vivo* competition assays. These strains also exhibited faster doubling times than the wild-type strain when grown in intestinal mucus, as well as in minimal medium supplemented with the sole carbon sources gluconate, arabinose, and ribose, which are all constituents of mucus. Overall, these results suggest that the $\Delta rpoN$ mutant *in vivo* phenotype is due in part to carbon utilization along with unidentified factors under the control of the RpoN regulon.

The role RpoN plays in gene regulation and host colonization has been studied in *V. cholerae* as well as in a number of other *Vibrio* species. In *V. cholerae*, the RpoN regulon encompasses nearly 500 genes, most of which are independent of flagellar synthesis (33). In addition to its role in the regulation of polar flagellum synthesis in *V. cholerae*, RpoN has been shown to play a role in growth on ammonium as the sole nitrogen source, the regulation of the type VI secretion system, and the regulation of quorum sensing. In addition, it was found that *rpoN* deletion mutants exhibited different growth patterns than the wild-type strain on a number of carbon sources, suggesting a role in carbon metabolism (26, 31–33, 35, 36, 62). Deletion of *rpoN* in *V. cholerae* also resulted in a strain that exhibited a nearly 30-fold decrease in competitive fitness compared to the wild-type strain using the cholera infant mouse model of colonization (32). FliAP has also been studied in *V. cholerae* and has been shown to regulate approximately 330 genes (33). The *fliAP* mutants in *V. cholerae* were nonmotile, demonstrated an increase in virulence gene expression and decreased biofilm production, and were able to differentially utilize various carbon sources compared to the wild-type strain (33). As with the *rpoN* deletion strains, *V. cholerae* that lacks a functional FliAP displays a reduced competitive index in the infant mouse model (54).

We recently introduced a new animal model for the study of *V. parahaemolyticus* colonization and survival within the host (28). This model relies on the streptomycin pretreatment of adult mice

to facilitate the colonization of the mice by *V. parahaemolyticus*. Through this model, we demonstrated that the two-component system ToxRS and the outer membrane protein OmpU were important survival factors for this organism *in vivo*, whereas T3SS-1 and T3SS-2 were not required for *in vivo* colonization (28). Here, we report that deletion of *rpoN*, *fliAP*, or a double deletion of *fliAP fliAL* results in strains that have increased fitness and a significant competitive advantage *in vivo*. This is in contrast to deletions of *rpoN* in *V. cholerae*, *V. anguillarum*, and *V. fischeri*, which all have deleterious effects on the ability of these strains to colonize their particular model host organism (32, 39, 40). However, it has been shown that loss of motility in biotype El Tor *V. cholerae* strains results in decreased CIs *in vivo*, whereas nonmotile classical biotype strains colonize as well as the wild-type strains (54, 63, 64).

There is evidence that a defect in motility can contribute to *in vivo* survival. Studies by Leatham et al. and Gauger et al. showed that a streptomycin-treated mouse model for *E. coli* invasiveness positively selected for motility-defective mutants in *E. coli* MG1665 (42, 65). Gauger et al. found that 30 to 40% of *E. coli* cells were nonmotile 3 days postinfection, and that number increased to 80 to 90% nonmotile cells 15 days postinfection (65). When reinfected into streptomycin-treated adult mice, these nonmotile strains were demonstrated to be better colonizers than motile *E. coli* MG1665 strains. Furthermore, nonmotile strains were able to grow 10 to 20% faster on mouse cecal mucus than their isogenic, motile, parent strains and 15 to 30% faster on sugars that are known to be present in the intestine (42, 65). This is similar to the data we present in this study on *V. parahaemolyticus*. We have shown that deletion of *rpoN* only causes a growth defect on minimal medium which lacks a glutamine source. We also demonstrated that the Δ*rpoN* strain has the ability to outcompete the wild-type strain during coinfections of streptomycin-treated adult mice. With this *in vivo* phenotype, the Δ*rpoN* strain exhibited higher growth rates in mouse intestinal mucus as well as in a number of sugars that are known to be present in the mouse intestine. In order to further our understanding of this phenotype, we constructed deletion mutants in the polar and lateral flagellar sigma factors, as well as a double deletion mutation in both sigma factors. These strains would retain the motility-defective phenotype but have a fully functioning RpoN. We found that strains carrying a deletion in the polar flagellum sigma factor, FliAP, or a defect in both flagellar systems were slightly better colonizers than the wild-type parent strains but not to the same extent as the *rpoN* mutant. These data suggest that loss of motility is not the cause of the increased fitness *in vivo*. As with the Δ*rpoN* strain, these strains also had higher growth rates on intestinal mucus and intestinal sugars than the wild-type strain. The Δ*fliAL* strain defective in lateral flagellum synthesis was the only mutant that could not significantly outcompete the wild type and had a doubling time similar to that of the wild type, suggesting that the *fliAL* gene plays no role in colonization or growth rates. The fact that Δ*fliAP* and Δ*fliAP*Δ*fliAL* strains colonized and doubled at similar rates further supports this hypothesis. It would appear that strains that are defective in the synthesis of the polar flagellum are better suited for an *in vivo* lifestyle. In *E. coli*, flagellar synthesis accounts for approximately 2% of the total energy cost of the cell (65, 66). Therefore, nonmotile strains, which no longer have to synthesize or expend energy to rotate the flagella, may use that excess energy for other cellular functions, causing them to grow at higher rates than the motile parent strain. This may be the case for the Δ*rpoN*,

Δ*fliAP*, and Δ*fliAP* Δ*fliAL* strains, as these are all defective for motility. In addition, when we analyzed the expression patterns of genes in the pathways for gluconate, ribose, and arabinose metabolism, we found that the three aforementioned mutants exhibited significantly higher expression ratios than the wild-type strain. This indicates that these pathways are repressed by either RpoN or FliAP and in the absence of these sigma factors, the pathways are derepressed, which leads to higher growth rates when these carbon sources are present in the growth medium. Recently, it was shown that lack of a functional polar flagellum does indeed cause global changes in *V. parahaemolyticus* (58), as cells grown on a surface (conditions where the polar flagellum is inhibited) or in mutant strains with defects in the polar flagellum exhibited alterations in nonmotility genes. However, genes relating to carbon utilization pathways were not found to be altered. It should be noted, however, that they examined expression in cells grown on heart infusion plates. Media such as LB and HI broth/plates typically do not contain fermentable carbon sources, which may have prevented the expression of carbon catabolism pathways (67, 68).

The derepression of the gluconate, ribose, and arabinose pathways exhibited in the Δ*rpoN*, Δ*fliAP*, and Δ*fliAP* Δ*fliAL* strains likely contributes to the higher growth rates in the aforementioned carbon sources as well as these strains' ability to outcompete the WBWlacZ strain in media containing mucus as the sole nutrition source. However, if this were solely the case, it would be expected that all three strains would outcompete the WBWlacZ strain equally *in vivo* as well. While the Δ*fliAP* and Δ*fliAP* Δ*fliAL* strains are similar in their ability to outcompete the WBWlacZ strain, the Δ*rpoN* strain outcompetes the WBWlacZ strain at a much greater magnitude, which indicates that there is more to this phenotype than just a loss of motility and ability to utilize carbon sources more efficiently. As mentioned previously, RpoN is a global regulator that controls the expression of a large number of nonmotility-associated genes (31–33). The Δ*rpoN* strain most likely is benefiting from some altered expression of these nonmotility genes in addition to the benefit seen in nonmotile but RpoN$^+$ strains (Δ*fliAP* and Δ*fliAP* Δ*fliAL* mutants). It would be of merit to examine the RpoN regulon further in *V. parahaemolyticus* to examine which other genes that are contributing to host colonization are differentially regulated by RpoN.

This is the first report on the ability of *V. parahaemolyticus* to utilize intestinal mucus as a sole carbon source. Mucus is a glycoprotein that contains fucose, galactose, gluconate, glucuronate, mannose, *N*-acetylglucosamine, *N*-acetylneuraminic acid, *N*-acetylgalactosamine, ribose, and arabinose as its major components (55, 56). Many of the pathways required to catabolize these compounds are present in *V. parahaemolyticus*. We have shown that this organism has the ability to grow in intestinal mucus and utilize a variety of sugar sources commonly found in intestinal mucus, specifically gluconate, mannose, ribose, and arabinose. Furthermore, strains that catabolize these nutritional sources at higher rates demonstrated higher fitness within the host. It will be interesting to examine further which catabolic pathways are more important during host survival and to see if this organism has preferred nutritional sources within the host.

REFERENCES

1. **Joseph SW, Colwell RR, Kaper JB.** 1982. *Vibrio parahaemolyticus* and related halophilic *Vibrios*. Crit. Rev. Microbiol. **10:**77–124. http://dx.doi.org/10.3109/10408418209113506.

2. **Kaneko T, Colwell RR.** 1973. Ecology of *Vibrio parahaemolyticus* in Chesapeake Bay. J. Bacteriol. **113:**24–32.

3. **Nordstrom JL, DePaola A.** 2003. Improved recovery of pathogenic *Vibrio parahaemolyticus* from oysters using colony hybridization following enrichment. J. Microbiol. Methods **52:**273–277. http://dx.doi.org/10.1016/S0167-7012(02)00188-4.

4. **Zimmerman AM, DePaola A, Bowers JC, Krantz JA, Nordstrom JL, Johnson CN, Grimes DJ.** 2007. Variability of total and pathogenic *Vibrio parahaemolyticus* densities in northern Gulf of Mexico water and oysters. Appl. Environ. Microbiol. **73:**7589–7596. http://dx.doi.org/10.1128/AEM.01700-07.

5. **Daniels NA, MacKinnon L, Bishop R, Altekruse S, Ray B, Hammond RM, Thompson S, Wilson S, Bean NH, Griffin PM, Slutsker L.** 2000. *Vibrio parahaemolyticus* infections in the United States, 1973–1998. J. Infect. Dis. **181:**1661–1666. http://dx.doi.org/10.1086/315459.

6. **Su YC, Liu C.** 2007. *Vibrio parahaemolyticus*: a concern of seafood safety. Food Microbiol. **24:**549–558. http://dx.doi.org/10.1016/j.fm.2007.01.005.

7. **Blackstone GM, Nordstrom JL, Vickery MC, Bowen MD, Meyer RF, DePaola A.** 2003. Detection of pathogenic *Vibrio parahaemolyticus* in oyster enrichments by real time PCR. J. Microbiol. Methods **53:**149–155. http://dx.doi.org/10.1016/S0167-7012(03)00020-4.

8. **McLaughlin JB, DePaola A, Bopp CA, Martinek KA, Napolilli NP, Allison CG, Murray SL, Thompson EC, Bird MM, Middaugh JP.** 2005. Outbreak of *Vibrio parahaemolyticus* gastroenteritis associated with Alaskan oysters. N. Engl. J. Med. **353:**1463–1470. http://dx.doi.org/10.1056/NEJMoa051594.

9. **Dabanch PJ, Herrero CD, Pavez AC, Veas PN, Braun JS, Porte TL.** 2009. *Vibrio parahaemolyticus* bacteremia: case report and literature review. Rev. Chilena Infectol. **26:**360–362.

10. **Lim TK, Stebbings AE.** 1999. Fulminant necrotising fasciitis caused by *Vibrio parahaemolyticus*. Singapore Med. J. **40:**596–597.

11. **Payinda G.** 2008. Necrotizing fasciitis due to *Vibrio parahaemolyticus*. N. Z. Med. J. **121:**99–101.

12. **Ralph A, Currie BJ.** 2007. *Vibrio vulnificus* and *V. parahaemolyticus* necrotising fasciitis in fishermen visiting an estuarine tropical northern Australian location. J. Infect. **54:**e111–e114. http://dx.doi.org/10.1016/j.jinf.2006.06.015.

13. **DePaola A, Ulaszek J, Kaysner CA, Tenge BJ, Nordstrom JL, Wells J, Puhr N, Gendel SM.** 2003. Molecular, serological, and virulence characteristics of *Vibrio parahaemolyticus* isolated from environmental, food, and clinical sources in North America and Asia. Appl. Environ. Microbiol. **69:**3999–4005. http://dx.doi.org/10.1128/AEM.69.7.3999-4005.2003.

14. **Johnson CN, Flowers AR, Young VC, Gonzalez-Escalona N, DePaola A, Noriea NF, III, Grimes DJ.** 2009. Genetic relatedness among tdh+ and trh+ *Vibrio parahaemolyticus* cultured from Gulf of Mexico oysters (Crassostrea virginica) and surrounding water and sediment. Microb. Ecol. **57:**437–443. http://dx.doi.org/10.1007/s00248-008-9418-3.

15. **Osawa R, Okitsu T, Morozumi H, Yamai S.** 1996. Occurrence of urease-positive *Vibrio parahaemolyticus* in Kanagawa, Japan, with specific reference to presence of thermostable direct hemolysin (TDH) and the TDH-related-hemolysin genes. Appl. Environ. Microbiol. **62:**725–727.

16. **Makino K, Oshima K, Kurokawa K, Yokoyama K, Uda T, Tagomori K, Iijima Y, Najima M, Nakano M, Yamashita A, Kubota Y, Kimura S, Yasunaga T, Honda T, Shinagawa H, Hattori M, Iida T.** 2003. Genome sequence of *Vibrio parahaemolyticus*: a pathogenic mechanism distinct from that of *V. cholerae*. Lancet **361:**743–749. http://dx.doi.org/10.1016/S0140-6736(03)12659-1.

17. **Park KS, Ono T, Rokuda M, Jang MH, Okada K, Iida T, Honda T.** 2004. Functional characterization of two type III secretion systems of *Vibrio parahaemolyticus*. Infect. Immun. **72:**6659–6665. http://dx.doi.org/10.1128/IAI.72.11.6659-6665.2004.

18. **Broberg CA, Zhang L, Gonzalez H, Laskowski-Arce MA, Orth K.** 2010. A *Vibrio* effector protein is an inositol phosphatase and disrupts host cell membrane integrity. Science **329:**1660–1662. http://dx.doi.org/10.1126/science.1192850.

19. **Burdette DL, Seemann J, Orth K.** 2009. *Vibrio* VopQ induces PI3-kinase-independent autophagy and antagonizes phagocytosis. Mol. Microbiol. **73:**639–649. http://dx.doi.org/10.1111/j.1365-2958.2009.06798.x.

20. **Burdette DL, Yarbrough ML, Orth K.** 2009. Not without cause: *Vibrio parahaemolyticus* induces acute autophagy and cell death. Autophagy **5:**100–102. http://dx.doi.org/10.4161/auto.5.1.7264.

21. **Gode-Potratz CJ, Chodur DM, McCarter LL.** 2010. Calcium and iron regulate swarming and type III secretion in *Vibrio parahaemolyticus*. J. Bacteriol. **192:**6025–6038. http://dx.doi.org/10.1128/JB.00654-10.

22. **Hiyoshi H, Kodama T, Iida T, Honda T.** 2010. Contribution of *Vibrio parahaemolyticus* virulence factors to cytotoxicity, enterotoxicity, and lethality in mice. Infect. Immun. **78:**1772–1780. http://dx.doi.org/10.1128/IAI.01051-09.

23. **Ritchie JM, Rui H, Zhou X, Iida T, Kodoma T, Ito S, Davis BM, Bronson RT, Waldor MK.** 2012. Inflammation and disintegration of intestinal villi in an experimental model for *Vibrio parahaemolyticus*-induced diarrhea. PLoS Pathog. **8:**e1002593. http://dx.doi.org/10.1371/journal.ppat.1002593.

24. **Boyd EF, Cohen AL, Naughton LM, Ussery DW, Binnewies TT, Stine OC, Parent MA.** 2008. Molecular analysis of the emergence of pandemic *Vibrio parahaemolyticus*. BMC Microbiol. **8:**110. http://dx.doi.org/10.1186/1471-2180-8-110.

25. **Hurley CC, Quirke A, Reen FJ, Boyd EF.** 2006. Four genomic islands that mark post-1995 pandemic *Vibrio parahaemolyticus* isolates. BMC Genomics **7:**104. http://dx.doi.org/10.1186/1471-2164-7-104.

26. **Izutsu K, Kurokawa K, Tashiro K, Kuhara S, Hayashi T, Honda T, Iida T.** 2008. Comparative genomic analysis using microarray demonstrates a strong correlation between the presence of the 80-kilobase pathogenicity island and pathogenicity in Kanagawa phenomenon-positive *Vibrio parahaemolyticus* strains. Infect. Immun. **76:**1016–1023. http://dx.doi.org/10.1128/IAI.01535-07.

27. **Pineyro P, Zhou X, Orfe LH, Friel PJ, Lahmers K, Call DR.** 2010. Development of two animal models to study the function of *Vibrio parahaemolyticus* type III secretion systems. Infect. Immun. **78:**4551–4559. http://dx.doi.org/10.1128/IAI.00461-10.

28. **Whitaker WB, Parent MA, Boyd A, Richards GP, Boyd EF.** 2012. The *Vibrio parahaemolyticus* ToxRS regulator is required for stress tolerance and colonization in a novel orogastric streptomycin-induced adult murine model. Infect. Immun. **80:**1834–1845. http://dx.doi.org/10.1128/IAI.06284-11.

29. **Gross CA, Chan C, Dombroski A, Gruber T, Sharp M, Tupy J, Young B.** 1998. The functional and regulatory roles of sigma factors in transcription. Cold Spring Harbor Symp. Quant. Biol. **63:**141–155. http://dx.doi.org/10.1101/sqb.1998.63.141.

30. **Reitzer L, Schneider BL.** 2001. Metabolic context and possible physiological themes of sigma(54)-dependent genes in *Escherichia coli*. Microbiol. Mol. Biol. Rev. **65:**422–444. http://dx.doi.org/10.1128/MMBR.65.3.422-444.2001.

31. **Dong TG, Mekalanos JJ.** 2012. Characterization of the RpoN regulon reveals differential regulation of T6SS and new flagellar operons in *Vibrio cholerae* O37 strain V52. Nucleic Acids Res. **40:**7766–7775. http://dx.doi.org/10.1093/nar/gks567.

32. **Klose KE, Mekalanos JJ.** 1998. Distinct roles of an alternative sigma factor during both free-swimming and colonizing phases of the *Vibrio cholerae* pathogenic cycle. Mol. Microbiol. **28:**501–520. http://dx.doi.org/10.1046/j.1365-2958.1998.00809.x.

33. **Syed KA, Beyhan S, Correa N, Queen J, Liu J, Peng F, Satchell KJ, Yildiz F, Klose KE.** 2009. The *Vibrio cholerae* flagellar regulatory hierarchy controls expression of virulence factors. J. Bacteriol. **191:**6555–6570. http://dx.doi.org/10.1128/JB.00949-09.

34. **Ishikawa T, Rompikuntal PK, Lindmark B, Milton DL, Wai SN.** 2009. Quorum sensing regulation of the two hcp alleles in *Vibrio cholerae* O1 strains. PLoS One **4:**e6734. http://dx.doi.org/10.1371/journal.pone.0006734.

35. **Williams SG, Varcoe LT, Attridge SR, Manning PA.** 1996. *Vibrio cholerae* Hcp, a secreted protein coregulated with HlyA. Infect. Immun. **64:**283–289.

36. **Yildiz FH, Liu XS, Heydorn A, Schoolnik GK.** 2004. Molecular analysis

of rugosity in a *Vibrio cholerae* O1 El Tor phase variant. Mol. Microbiol. **53:**497–515. http://dx.doi.org/10.1111/j.1365-2958.2004.04154.x.

37. **Klose KE, Novik V, Mekalanos JJ.** 1998. Identification of multiple sigma54-dependent transcriptional activators in *Vibrio cholerae*. J. Bacteriol. **180:**5256–5259.

38. **Kawagishi I, Nakada M, Nishioka N, Homma M.** 1997. Cloning of a *Vibrio alginolyticus rpoN* gene that is required for polar flagellar formation. J. Bacteriol. **179:**6851–6854.

39. **O'Toole R, Milton DL, Horstedt P, Wolf-Watz H.** 1997. RpoN of the fish pathogen *Vibrio* (*Listonella*) *anguillarum* is essential for flagellum production and virulence by the water-borne but not intraperitoneal route of inoculation. Microbiology **143**(Part 12)**:**3849–3859. http://dx.doi.org/10.1099/00221287-143-12-3849.

40. **Wolfe AJ, Millikan DS, Campbell JM, Visick KL.** 2004. *Vibrio fischeri* sigma54 controls motility, biofilm formation, luminescence, and colonization. Appl. Environ. Microbiol. **70:**2520–2524. http://dx.doi.org/10.1128/AEM.70.4.2520-2524.2004.

41. **Whitaker WB, Parent MA, Naughton LM, Richards GP, Blumerman SL, Boyd EF.** 2010. Modulation of responses of *Vibrio parahaemolyticus* O3:K6 to pH and temperature stresses by growth at different salt concentrations. Appl. Environ. Microbiol. **76:**4720–4729. http://dx.doi.org/10.1128/AEM.00474-10.

42. **Leatham MP, Stevenson SJ, Gauger EJ, Krogfelt KA, Lins JJ, Haddock TL, Autieri SM, Conway T, Cohen PS.** 2005. Mouse intestine selects nonmotile *flhDC* mutants of *Escherichia coli* MG1655 with increased colonizing ability and better utilization of carbon sources. Infect. Immun. **73:**8039–8049. http://dx.doi.org/10.1128/IAI.73.12.8039-8049.2005.

43. **Cohen PS, Laux DC.** 1995. Bacterial adhesion to and penetration of intestinal mucus in vitro. Methods Enzymol. **253:**309–314.

44. **Pfaffl MW.** 2001. A new mathematical model for relative quantification in real-time RT-PCR. Nucleic Acids Res. **29:**e45. http://dx.doi.org/10.1093/nar/29.9.e45.

45. **Arous S, Buchrieser C, Folio P, Glaser P, Namane A, Hebraud M, Hechard Y.** 2004. Global analysis of gene expression in an rpoN mutant of *Listeria monocytogenes*. Microbiology **150:**1581–1590. http://dx.doi.org/10.1099/mic.0.26860-0.

46. **Totten PA, Lara JC, Lory S.** 1990. The *rpoN* gene product of *Pseudomonas aeruginosa* is required for expression of diverse genes, including the flagellin gene. J. Bacteriol. **172:**389–396.

47. **Klose KE, Mekalanos JJ.** 1997. Simultaneous prevention of glutamine synthesis and high-affinity transport attenuates *Salmonella typhimurium* virulence. Infect. Immun. **65:**587–596.

48. **Reitzer LJ, Bueno R, Cheng WD, Abrams SA, Rothstein DM, Hunt TP, Tyler B, Magasanik B.** 1987. Mutations that create new promoters suppress the sigma 54 dependence of *glnA* transcription in *Escherichia coli*. J. Bacteriol. **169:**4279–4284.

49. **Kim YK, McCarter LL.** 2000. Analysis of the polar flagellar gene system of *Vibrio parahaemolyticus*. J. Bacteriol. **182:**3693–3704. http://dx.doi.org/10.1128/JB.182.13.3693-3704.2000.

50. **Stewart BJ, McCarter LL.** 2003. Lateral flagellar gene system of *Vibrio parahaemolyticus*. J. Bacteriol. **185:**4508–4518. http://dx.doi.org/10.1128/JB.185.15.4508-4518.2003.

51. **Eaton KA, Morgan DR, Krakowka S.** 1992. Motility as a factor in the colonisation of gnotobiotic piglets by *Helicobacter pylori*. J. Med. Microbiol. **37:**123–127. http://dx.doi.org/10.1099/00222615-37-2-123.

52. **Josenhans C, Suerbaum S.** 2002. The role of motility as a virulence factor in bacteria. Int. J. Med. Microbiol. **291:**605–614. http://dx.doi.org/10.1078/1438-4221-00173.

53. **Lane MC, Lockatell V, Monterosso G, Lamphier D, Weinert J, Hebel JR, Johnson DE, Mobley HL.** 2005. Role of motility in the colonization of

54. **Liu Z, Miyashiro T, Tsou A, Hsiao A, Goulian M, Zhu J.** 2008. Mucosal penetration primes *Vibrio cholerae* for host colonization by repressing quorum sensing. Proc. Natl. Acad. Sci. U. S. A. **105:**9769–9774. http://dx.doi.org/10.1073/pnas.0802241105.

55. **Chang DE, Smalley DJ, Tucker DL, Leatham MP, Norris WE, Stevenson SJ, Anderson AB, Grissom JE, Laux DC, Cohen PS, Conway T.** 2004. Carbon nutrition of *Escherichia coli* in the mouse intestine. Proc. Natl. Acad. Sci. U. S. A. **101:**7427–7432. http://dx.doi.org/10.1073/pnas.0307888101.

56. **Peekhaus N, Conway T.** 1998. What's for dinner? Entner-Doudoroff metabolism in *Escherichia coli*. J. Bacteriol. **180:**3495–3502.

57. **McCarter LL.** 2001. Polar flagellar motility of the *Vibrionaceae*. Microbiol. Mol. Biol. Rev. **65:**445–462. http://dx.doi.org/10.1128/MMBR.65.3.445-462.2001.

58. **Gode-Potratz CJ, Kustusch RJ, Breheny PJ, Weiss DS, McCarter LL.** 2011. Surface sensing in *Vibrio parahaemolyticus* triggers a programme of gene expression that promotes colonization and virulence. Mol. Microbiol. **79:**240–263. http://dx.doi.org/10.1111/j.1365-2958.2010.07445.x.

59. **McCarter LL, Wright ME.** 1993. Identification of genes encoding components of the swarmer cell flagellar motor and propeller and a sigma factor controlling differentiation of *Vibrio parahaemolyticus*. J. Bacteriol. **175:**3361–3371.

60. **Maltby R, Leatham-Jensen MP, Gibson T, Cohen PS, Conway T.** 2013. Nutritional basis for colonization resistance by human commensal *Escherichia coli* strains HS and Nissle 1917 against *E. coli* O157:H7 in the mouse intestine. PLoS One **8:**e53957. http://dx.doi.org/10.1371/journal.pone.0053957.

61. **Stecher B, Hardt WD.** 2011. Mechanisms controlling pathogen colonization of the gut. Curr. Opin. Microbiol. **14:**82–91. http://dx.doi.org/10.1016/j.mib.2010.10.003.

62. **Lenz DH, Miller MB, Zhu J, Kulkarni RV, Bassler BL.** 2005. CsrA and three redundant small RNAs regulate quorum sensing in *Vibrio cholerae*. Mol. Microbiol. **58:**1186–1202. http://dx.doi.org/10.1111/j.1365-2958.2005.04902.x.

63. **Gardel CL, Mekalanos JJ.** 1996. Alterations in *Vibrio cholerae* motility phenotypes correlate with changes in virulence factor expression. Infect. Immun. **64:**2246–2255.

64. **Lee SH, Butler SM, Camilli A.** 2001. Selection for in vivo regulators of bacterial virulence. Proc. Natl. Acad. Sci. U. S. A. **98:**6889–6894. http://dx.doi.org/10.1073/pnas.111581598.

65. **Gauger EJ, Leatham MP, Mercado-Lubo R, Laux DC, Conway T, Cohen PS.** 2007. Role of motility and the *flhDC* operon in *Escherichia coli* MG1655 colonization of the mouse intestine. Infect. Immun. **75:**3315–3324. http://dx.doi.org/10.1128/IAI.00052-07.

66. **Macnab R.** 1996. Flagella and motility, p 123–145. *In* Neidhardt FC, Curtiss R, III, Ingraham JL, Lin ECC, Low KB, Magasanik B, Reznikoff WS, Riley M, Schaechter M, Umbarger HE (ed), *Escherichia coli* and *Salmonella*: cellular and molecular biology, 2nd ed, vol 1. ASM Press, Washington, DC.

67. **Haque RU, Baldwin JN.** 1964. Purification and properties of *Staphylococcal* beta-hemolysin. I. Production of beta-hemolysin. J. Bacteriol. **88:**1304–1309.

68. **Sezonov G, Joseleau-Petit D, D'Ari R.** 2007. *Escherichia coli* physiology in Luria-Bertani broth. J. Bacteriol. **189:**8746–8749. http://dx.doi.org/10.1128/JB.01368-07.

69. **Philippe N, Alcaraz JP, Coursange E, Geiselmann J, Schneider D.** 2004. Improvement of pCVD442, a suicide plasmid for gene allele exchange in bacteria. Plasmid **51:**246–255. http://dx.doi.org/10.1016/j.plasmid.2004.02.003.